Desalination and Water Treatment
www.deswater.com

43 (2012) 76–83
April

1944-3994/1944-3986 © 2012 Desalination Publications. All rights reserved
doi: 10.1080/19443994.2012.672205

Taylor & Francis
Taylor & Francis Group

Analysis of an evaporation–condensation desalination system in vacuum driven by geothermal energy

Penghui Gao*, Guoqing Zhou

State Key Laboratory for GeoMechanics and Deep Underground Engineering, School of Architecture and Civil Engineering, China University of Mining and Technology, Xuzhou, Jiangsu 221116, China
Tel. +86 516 83882193; Fax: +86 516 83885478; email: gaopenghui2004@126.com

Received 17 March 2011; Accepted 2 February 2012

ABSTRACT

A new multiple-effect desalination system in vacuum powered by geothermal energy considered as clean and renewable natural energy resource is proposed. Every effect includes an evaporator and a condenser which are composed of heat pipes to work in vacuum. The performance of one effect was studied by employing a mathematical model based on energy and mass balance equations. The performance of system was evaluated through several indicators: performance ratio, heat transfer area of per-water production, and coefficient of performance. The results showed that freshwater production ratio increased with the geothermal water flow and geothermal temperature, but could not increase with the condensation vacuum enhancing. In conclusion, the analysis has shown that geothermal resource in the temperature range of 50–100°C has a good potential to power seawater vacuum desalination system. It would be beneficial for people in the areas with abundant seawater/brackish water resources and good geothermal conditions.

Keywords: Geothermal energy; Desalination; Heat pipe

1. Introduction

Part of the world is experiencing a water crisis [1], and the United Nations Environment Program has estimated that from now up to 2,027 approximately one-third of the world's population will suffer serious water scarcity problems. Desalination, that is the separation of saline seawater/brackish water into two streams: a freshwater stream containing a low concentration of dissolved salts and a concentrated brine stream, has been as an important approach to get freshwater. Today, some countries depend on desalination technologies for the purpose of meeting their freshwater requirements. In particular, in the Middle East, in countries such as Saudi Arabia, United Arab Emirates, and Kuwait, seawater desalination is a vital and dependable freshwater resource [2]. Desalination technologies that have been developed over the years are thermal distillation, membrane separation, freezing, and electrodialysis [3–7]. Now, the most widely used desalination technologies are multi-stage flash distillation (MSF), multiple-effect distillation (MED), and reverse osmosis (RO) [8].

Various renewable energy sources such as solar energy, geothermal energy, and wind power are used in desalination to reduce the fossil fuels consumption and to protect the environment. Patricia et al. [9] studied a solar multi-effect desalination plant and analyzed the heat transfer characteristic in the system. Mahmoudi et al. [10] presented a desalination system powered by solar and wind energy. Mahmoudi et al. [11] proposed a new brackish water

*Corresponding author.

greenhouse desalination unit powered by geothermal energy and assessed geothermal desalination. Jouhara et al. [12] brought to light a new concept for nuclear desalination system based on heat pipe technology and discussed the anticipated reduction in the tritium level resulting from the use of heat pipes. Tanaka and Park [13] analyzed theoretically a distillation utilizing waste heat from a portable electric generator by means of a heat pipe. The system could produce 20 kg of distilled water in 2 h of operation. Having the virtue of cleanness, less pollution to the environment, and reserves hugeness, geothermal energy is now being exploited and used to generate electricity and heat for heating processes and refrigeration system. Some examples of application are Reykjavik power station of Iceland, Queensland electricity plant, Nevada geothermal power station, Yangbajing power station of China, and Tianjin geothermal heating system of China.

This paper present a new vacuum evaporation–condensation desalination system driven by geothermal energy. The desalination process is working in the vacuum to debase the boiling point temperature of seawater/brackish water and powered by geothermal energy mainly. The seawater/brackish water evaporation and the water vapor condensation take place on the surface of heat pipe. The influence of different parameters on water production will be investigated to assess the advantages of using geothermal sources to power the seawater/brackish water desalination system.

2. Process equipment

Geothermal resources are classified according to their reservoir enthalpy/temperature: low (<100°C), medium (100–150°C), and high temperatures (>150°C). Considering evaporation in the vacuum, the boiling point temperature of liquid reduces to about 50°C when the pressure is 0.011 MPa. So, geothermal energy could play an important role as a source of energy for low temperature desalination system.

An evaporation–condensation desalination system in vacuum powered by geothermal energy is devised. The schematic diagram of the system is shown in Fig. 1. For the system could have many effects, the centerline denotes the ellipsis of other effects. Every effect includes an evaporator and a condenser which are composed of heat pipes and works in the vacuum. In evaporator of the first effect, one side of heat pipes is heated by the geothermal hot water and the heat is transferred by the heat pipe to the other side of the heat pipe on which seawater is sprayed to evaporate. The water vapor produced from here is pumped into the condenser of the next effect to get the freshwater and to provide heat to evaporate the next effect spray seawater.

A portion of vapor from the evaporator exchanges heat with feed seawater before it is sprayed. The other vapor is carried out to the next condenser to produce freshwater, simultaneously, it is as heat source to evaporate seawater. The new evaporation vapor is carried to the neighboring effect to begin a new process. The

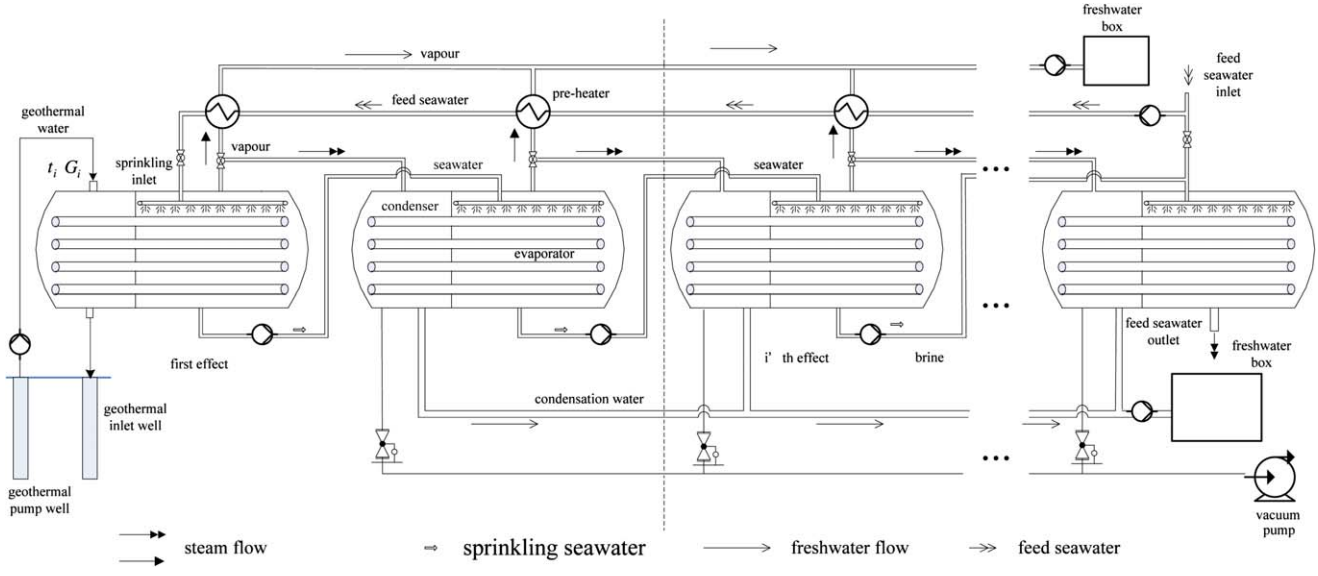

Fig. 1. Principle and schematic diagram of vacuum evaporation–condensation desalination system powered by geothermal energy.

schematic diagram of one effect is shown in Fig. 2. Every effect is operating in the given negative pressure to ensure evaporation temperature low and to keep temperature difference in every effect. Heat pipes make the evaporation process and condensation process to progress respectively. The vacuum of evaporator and condenser is gained by the vacuum pump.

3. Theoretical model

A nine-effect desalination system driven by the geothermal energy is analyzed in this paper. In the design, the heat pipe's diameter is 25 mm and the length of the heat pipe is 1500 mm. Heat pipes' disposal (row × line) is 36 × 3. Every effect operation parameter of the desalination system is shown in Table 1.

The mathematical model is developed according to energy and mass balance equations. It includes energy conservation, mass conservation, and heat exchanger energy balance of evaporation and condensation processes.

In order to calculate the system, certain idealizations need to be made.

- The system works in steady-state conditions, and thus all processes can be analyzed as steady-flow processes.
- The system is assumed to be adiabatic and the evaporation and condensation processes are taking place at the boiling point of the fluid.

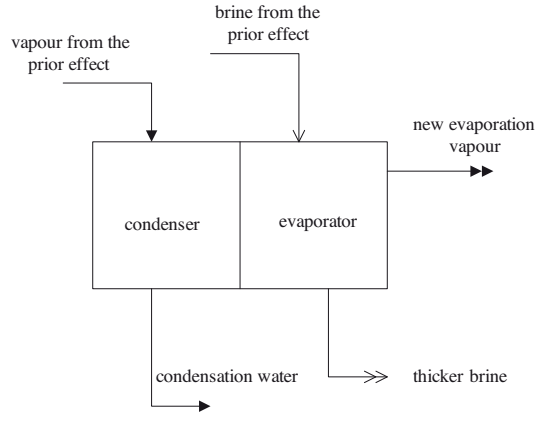

Fig. 2. The schematic diagram of one effect.

- The properties of water are considered constant here.

3.1. Theoretical model of the first effect

3.1.1. Geothermal energy balance equation

Geothermal hot water is pumped into the side of the evaporate and its heat is transferred to the other side by the heat pipe to evaporate. The energy equation is as follows:

$$q_{\mathrm{ge}} = q_{\mathrm{sew}} \tag{1}$$

It can be denoted:

$$m_{\mathrm{gew}} c_{\mathrm{p}} (t_{\mathrm{gewi}} - t_{\mathrm{gewo}}) = m'_{\mathrm{sew}} \cdot r + m''_{sew} c'_{p} (t_{\mathrm{sewo}} - t_{\mathrm{sewi}}) \tag{2}$$

3.1.2. Heat transfer equations of evaporation and condensation processes

(I) Heat transfer equation of evaporation is:

$$m'_{\mathrm{sew}} \cdot r + m''_{\mathrm{sew}} c'_{\mathrm{p}} (t_{\mathrm{sewo}} - t_{\mathrm{sewi}}) = A_{\mathrm{ev}} \cdot h_{\mathrm{ev}} \cdot \Delta\theta \tag{3}$$

In Eq. (3), h_{ev} is the heat transfer coefficient of evaporation [14,15], which is:

$$h_{\mathrm{ev}} = N^{0.032} 0.0175 k_{\mathrm{f}} \left(\frac{g}{\upsilon_{\mathrm{f}}^2}\right)^{\frac{1}{3}} \left(\frac{4\Gamma}{\mu_{\mathrm{f}}}\right)^{0.24} \left(\frac{\upsilon_{\mathrm{f}}}{a_{\mathrm{f}}}\right)^{0.66} \cdot \left(\frac{t_{\mathrm{w}}}{t_{\mathrm{f}}}\right)^{1.505} \cdot \mathrm{Pr}_{\mathrm{f}}^{0.8271} \cdot \left(\frac{p_{\mathrm{v}}}{p_{\mathrm{b}}}\right)^{0.1277} \tag{4}$$

(II) Heat transfer equation of condensation is:

$$m_{\mathrm{va}} \cdot r = A_{\mathrm{cond}} \cdot h_{\mathrm{cond}} \cdot \Delta\theta' \tag{5}$$

In Eq. (4), h_{cond} is the heat transfer coefficient of condensation [14], which is:

$$h_{\mathrm{cond}} = N^{-0.165} [1 + 0.2\zeta(N-1)] \cdot 0.541 \left[\frac{g r \rho_l^2 \lambda_l^3}{\mu_l (t_{\mathrm{s}} - t_{\mathrm{w}})}\right]^{1/4} \cdot \mathrm{Pr}_f^{0.961} \cdot \left(\frac{p_{\mathrm{v}}}{p_{\mathrm{b}}}\right)^{-0.02} \tag{6}$$

Table 1
Every effect operation parameter of the desalination system

Effect number	1	2	3	4	5	6	7	8	9
Evaporating temperature (°C)	69.1	67.3	65.3	62.2	58.8	56.5	53.2	50.5	47.5
Pressure (MPa)	0.0300	0.0278	0.0253	0.0221	0.0189	0.0170	0.0145	0.0129	0.011

3.1.3. Mass balance equations

For the evaporator, the mass balance equation is described as:

$$m_{\text{sew}} = m'_{\text{sew}} + m''_{\text{sew}} \tag{7}$$

where m'_{sew} is the vapor quantity produced by evaporation and m''_{sew} is the un-evaporation seawater quantity.

The salt quantity balance equation is:

$$m_{\text{sew}} \cdot C_i = m''_{\text{sew}} \cdot C_{\text{out}} \tag{8}$$

3.2. Calculation model of one effect from the second effect to the $(N-1)$th effect

The mass balance equation is listed as:

$$G_{i-1} = G_i + W_i \tag{9}$$

In the formula, G_{i-1} is the inlet seawater flow of the effect, kg/h; W_i is the steam produced from this effect, kg/h; and G_i is the outlet seawater flow of the effect, kg/h.

Salt balance equation is listed as:

$$G_i \cdot C_i = G_{i-1} \cdot C_{i-1} \tag{10}$$

In the formula, C_i and C_{i-1} are the outlet and inlet brine consistencies, %.

The energy balance equation is:

$$W_i \cdot r_i = [D_{i-1} \cdot r_{i-1} + G_{i-1} \cdot C_{p(i-1)} \cdot (T_{i-1} - T_i)] \cdot \eta \tag{11}$$

In the formula, D is the steam mass flow which is produced by the prior effect, r_i is the steam latent heat of the effect, J/Kg, and η is the thermal efficiency of every effect.

The brine boiling point of the effect is:

$$T_i = T_i + \text{BPE}(C_i, T_i) \tag{12}$$

In the formula, boiling point elevation (BPE) is the seawater boiling point [16], which is:

$$\begin{aligned}\text{BPE}(C,T) = {} & (5.28764 \times 10^{-2} + 8.2603 \times 10^{-4}T - 3.15082 \\ & \times 10^{-8}T^2)C + (3.20553 \times 10^{-3} - 1.44367 \\ & \times 10^{-5}T - 1.84416 \times 10^{-7}T^2)C^2\end{aligned}$$

The steam temperature of the effect is:

$$J_{i-1} = T_{i-1} - \text{BPE}(C_{i-1}, T_{i-1}) \tag{13}$$

The temperature difference of the effect is:

$$S_i = J_{i-1} - T_i \tag{14}$$

The consuming quality for pre-heater is:

$$W_{0i} = \frac{G_0 \cdot C_{\text{p}i} \cdot (T_i - T_{i+1})}{r_i} \tag{15}$$

The heat transfer formula is:

$$\begin{aligned}&D_{i-1} \times r_{i-1} + C_{\text{p}(i-1)} \times G_{i-1} \times (T_{i-1} - T_i) \\ &\quad = A_i \times k_i \times (T_{i-1} - T_i)\end{aligned} \tag{16}$$

In Formula (16), A_i is the falling film evaporation area of heat pipe and k_i is the total heat transfer coefficient of the effect which is the base of the falling film evaporation area of the heat pipe.

$$k_i = \frac{1}{\frac{1}{h_{1i}} + \frac{d_i \cdot \ln(\frac{d_i}{d_i - \delta_i})}{2\lambda_i} + \frac{l_{1i} \cdot d \cdot \ln(\frac{d_i}{d_i - \delta_i})}{2\lambda_i \cdot l_{2i}} + \frac{l_{1i}}{h_{2i} \cdot l_{2i}} + R_{\text{f}i}} \tag{17}$$

In Formula (17), l_1 is the heated length of the heat pipe, l_2 is the heat discharged length of the heat pipe, and h_{1i} is the heated heat transfer coefficient of the heat pipe [14,17], which is:

$$h_{1i} = \begin{cases} C\text{Re}^n \,\text{Pr}^{1/3} & \text{(a)} \\ 0.541\left[\frac{gr\rho_l^2\lambda_l^3}{\eta_l(t_s - t_w)}\right]^{1/4} \cdot \text{Pr}_{\text{f}}^{0.961} \cdot \left(\frac{p_v}{p_b}\right)^{-0.02} & \text{(b)} \end{cases} \tag{18}$$

h_{2i} is the discharged heat transfer coefficient of the heat pipe [3,5], which is:

$$h_{2i} = \begin{cases} \lambda \Big/ \left[\frac{ax\mu^{\frac{2}{3}}}{8(\rho_l - \rho_v)^{\frac{1}{3}} g^{\frac{2}{3}} (3m)^{\frac{1}{3}} \sin^{\frac{2}{3}}(\frac{\gamma}{R})}\right]^{\frac{1}{3}} & \text{(a)} \\ C\text{Re}^n \,\text{Pr}^{1/3} & \text{(b)} \end{cases} \tag{19}$$

The heated steam quality for heating the next effect is:

$$D_i = W_i - W_{0i} \tag{20}$$

3.3. Evaluation parameter

(1) Performance ratio

It is calculated by the formula:

$$P_w = \frac{M}{D_0} \tag{21}$$

where M is the water production rate of system and D_0 is the vapor quantity that is needed to heat. Here, D_0 is equivalent to the heat quantity with geothermal water quantity.

(2) Area of per-water production

$$\psi = \frac{A_{\text{all}}}{M} \tag{22}$$

where A_{all} is the heat transfer total area of the desalination system.

(3) Coefficient of performance (COP)

$$\text{COP} = \frac{q_e}{q_{ge}} \tag{23}$$

where q_e is the heat of evaporation from effects and q_{ge} is the geothermal heat.

4. Simulation results

4.1. Performance of one effect

The performance of one effect is studied in the different working conditions and temperature of geothermal source based on the energy and mass balance equations mentioned above. The geothermal source temperature, the geothermal water flow, and the vacuum of evaporation and condensation processes are analyzed to make clear the performance.

Fig. 3 shows that the vapor production ratio in the evaporator varies with geothermal water flow in different vacuum when the geothermal source temperature is 58°C, the spray density is 0.25 kg/(m s), and the spray seawater temperature is 38°C. From the figure, the vapor production ratio increases with the vacuum increasing. In given vacuum, the vapor production ratio increases with the geothermal water flow increasing.

Fig. 4 shows the variation of the vapor production ratio with geothermal water flow in different spray density when the geothermal source temperature is 58°C, the vacuum is 0.07 MPa, and the spray seawater temperature is 38°C. From the figure, the vapor production ratio increases with the spray density increasing. In a given spray density, the vapor production ratio increases with the geothermal water flow increasing.

The effect of condensation vacuum on the freshwater production at different vapor flow that are 100, 125, and 150 kg/h, respectively, is illustrated in Fig. 5.

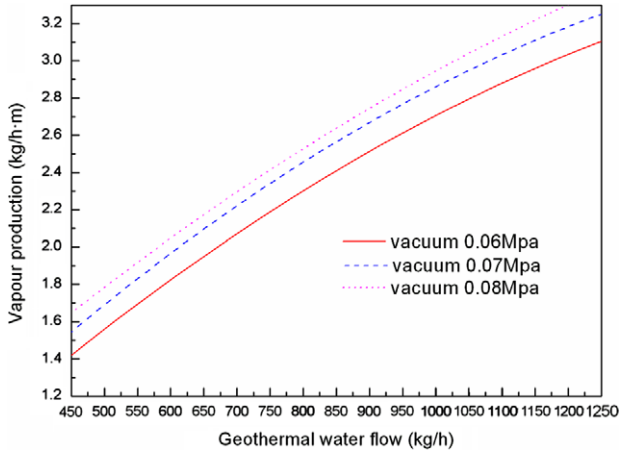

Fig. 3. Variation of vapor production ratio with geothermal water flow at different vacuum.

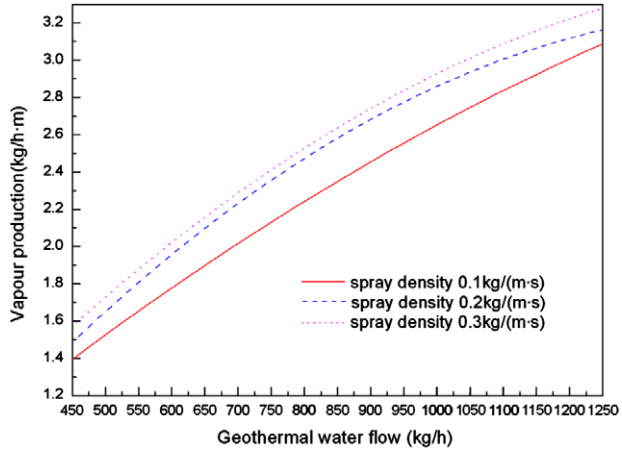

Fig. 4. Variation of vapor production ratio with geothermal water flow at different spray density.

The working conditions are that the temperature of vapor is 60°C, the cool water flow is 1,500 kg/h, and the temperature of cool water is 18°C. It can be seen that the water production reduces with the condensation vacuum increasing because the liquid film outside of the heat pipe becomes thicker as the condensation in bigger vacuum and the heat transfer obstruct increases. So, the heat transfer process is weakened and the condensation mass reduces. But, at definite condensation vacuum, the water production increases with the vapor flow increasing.

The effect of inlet temperature of cool water on the freshwater production at different cool water flow that they are 2,000, 3,000, and 4,000 kg/h, respectively, is illustrated in Fig. 6. It can be seen that the water production ratio reduces with the inlet temperature of cool water increasing. The reason is that the inlet

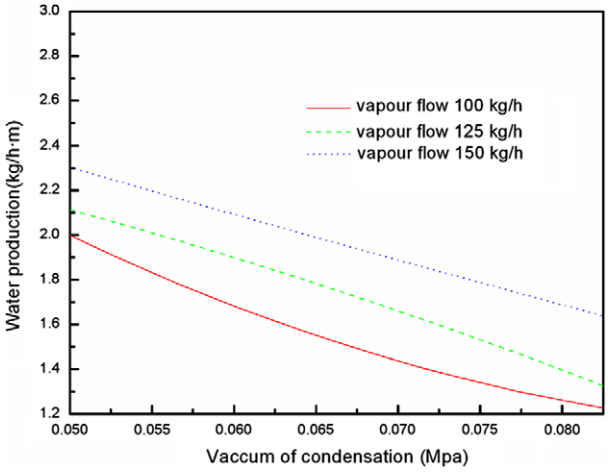

Fig. 5. The effect of condensation vacuum on the freshwater production at different vapor flow.

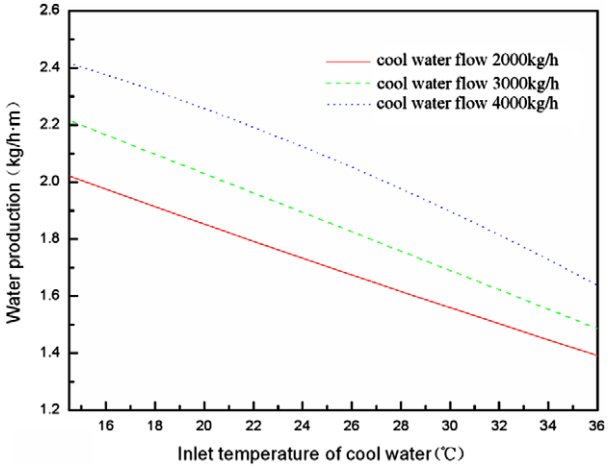

Fig. 6. Effect of inlet temperature of cool water on the freshwater production at different cool water flow.

temperature of cool water is improved and the cool quantity from the cool water is reduced. At the same inlet temperature of cool water, the water production ratio increases with the cool water flow increasing.

4.2. Performance of system

The performance of system is analyzed and evaluated by parameters of performance ratio, area of per-water production, and COP.

The variations of performance ratio of system with geothermal water flow rate in three different geothermal water temperatures of 60, 80, and 100°C are shown in Fig. 7. The performance ratio of system increases with the geothermal water flow rate. The performance ratio of geothermal water temperature

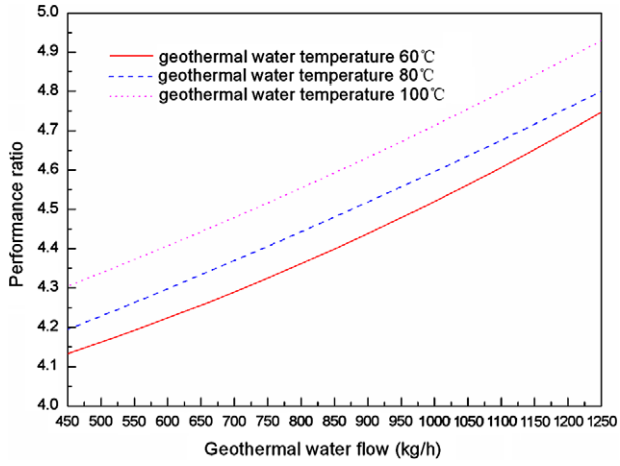

Fig. 7. Variations of performance ratio of system with geothermal water flow rate.

100°C is larger than geothermal water temperatures of 80 and 60°C. This is because the higher geothermal water temperature and the flow rate can provide more and higher grade heat to produce the vapor, thus making the system produce more freshwater.

The variations of performance ratio of system with the number of effects in three different geothermal water temperatures of 60, 80, and 100°C are shown in Fig. 8, when the geothermal water flow rate is 1,000 kg/h. From the figure, the performance ratio increases with the effect number and the performance ratio variation tendency in three different geothermal water temperatures of 60, 80, and 100°C is similar and nearly equal. In practice, the effect number of system can make six or more effects.

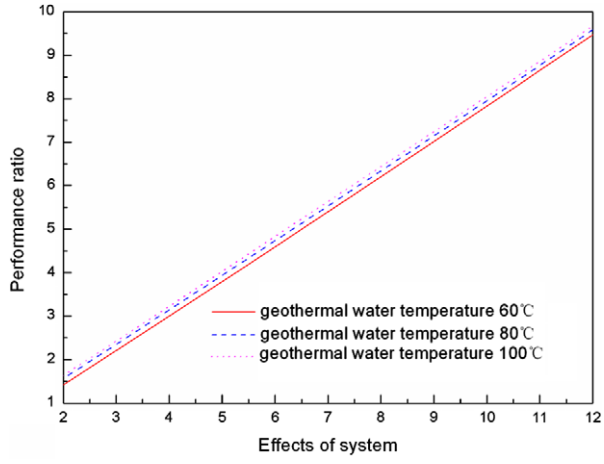

Fig. 8. Variations of performance ratio of system with effect number.

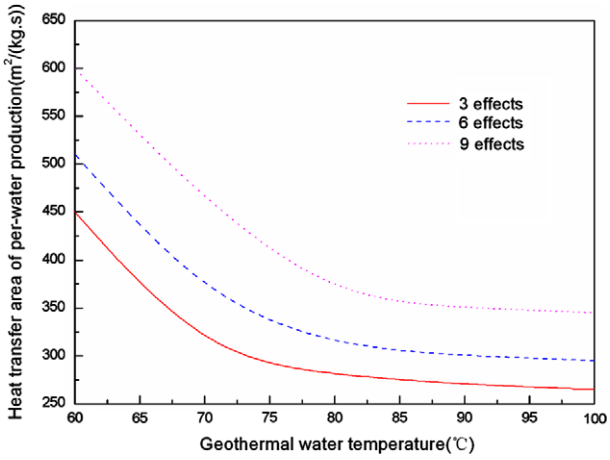

Fig. 9. Variations of heat transfer area of per-water production with geothermal water temperature.

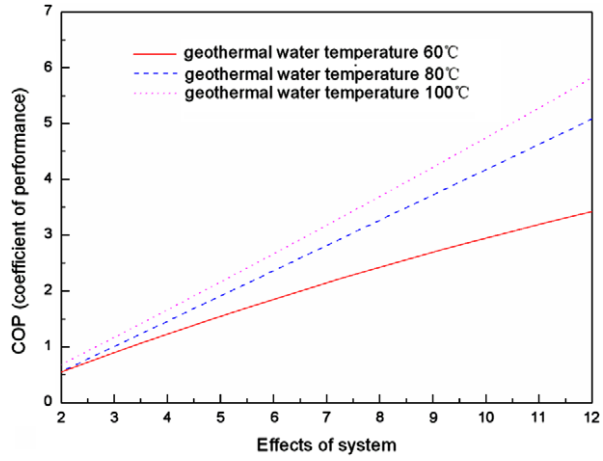

Fig. 10. Variations of COP with effect number.

The variations of heat transfer area of per-water production with geothermal water temperature in three different effects of 3, 6, and 9 are shown in Fig. 9, when the geothermal water flow rate is 1,000 kg/h. From Fig. 9, the heat transfer area decreases with geothermal water temperature. This is because that higher geothermal water temperature can make the temperature difference of heat transfer increase and favor heat transfer. The heat transfer area increases with the effect number. The reason is that temperature difference of more effects is decreased when the temperatures of geothermal water and feed seawater are determinate.

The COP with the effect number in three different geothermal water temperatures of 60, 80, and 100°C are shown in Fig. 10, when the geothermal water flow rate is 1,000 kg/h. The COP increases with the effect number increasing and is larger than 1.0 when the effect number is larger than 4, since the geothermal energy is utilized gradually in the succeeding effects of the desalination system. The COP is larger at a geothermal water temperature of 100°C than others at the geothermal water temperatures of 60 and 80°C. This is because that higher temperature of geothermal water can provide higher grade heat and drive the system to produce more vapor and obtain more freshwater.

5. Conclusions

An evaporation–condensation desalination system in vacuum powered by geothermal energy is devised. A calculation model of system is developed to analyze and evaluate the performance of system.

The following conclusions have been concluded:

- Geothermal resource is available in the temperature range of 50–100°C and has a good potential to power seawater vacuum desalination system.
- Freshwater production ratio increases with the geothermal water flow, evaporation vacuum, and spray density. It is advertent that the freshwater production ratio does not increase with the condensation vacuum enhancing.
- In order to produce more freshwater, the lower cooling water temperature helps in freshwater production. Higher geothermal temperature and bigger geothermal flow helps in freshwater production.
- Effect number is obtained from a compromise between performance ratio, heat transfer area of per-water production and COP. The reason is that the performance ratio and the COP of system increase with the effect number, but the heat transfer area of per-water production decreases with the effect number increasing when the temperatures of geothermal water and feed seawater are determinate.

In conclusion, this analysis has shown that there is great potential for use of geothermal energy to power the seawater/brackish water desalination units that it can help people in regions where there is a good geothermal resource.

Acknowledgments

The work was supported by the Chinese Foundation Committee of Nature and Science (Project No. 51106176), China Postdoctoral Science Foundation (Project No. 20110490042), Fundamental Research Funds for the Central Universities (Project No.

2010QNA44), and the State Key Laboratory for GeoMechanics and Deep Underground Engineering of China University of Mining and Technology, under Postdoctoral Project No. 1001.

Symbols

q	—	heat transfer rate, kW
c_p	—	specific heat capacity, J/(kg K)
m	—	mass flow rate, kg/s
t	—	temperature, °C
r	—	latent heat, J/kg
N	—	pipe number
k	—	heat transfer coefficient, W/(mk)
v	—	kinetic viscosity, m^2/s
μ	—	dynamic viscosity, kg/(m s)
Γ	—	spray density, kg/(m s)
a	—	thermal diffusion coefficient, m^2/s
P	—	pressure, MPa
ξ	—	dimensionless coefficient
λ	—	thermal conductivity, W/(m °C)
P_r	—	Prandtl number, dimensionless
C	—	salinity, g/kg
$\Delta\theta$	—	temperature difference, °C
Subscripts		
ge	—	geothermal
gew	—	geothermal hot water
gewi	—	inlet of geothermal hot water
gewo	—	outlet of geothermal hot water
sew	—	seawater
sewo	—	outlet of seawater
sewi	—	inlet of seawater
ev	—	evaporation
va	—	water vapor
w	—	wall
f	—	liquid

References

[1] Riccardo Petrella, The Water Manifesto, Arguments for a World Water Contract, Zed Books, London, 2001.
[2] L.I. Alawadhi, Regional Report on Desalination-GCC Countries, in: *Proceedings of the IDA World Congress on Desalination and Water Reuse*, March 8–13, Manama, Bahrain, 2002, pp. 126–135.
[3] E.D. Howe, Fundamentals of Water Desalination, Marcel Dekker, New York, NY, 1974.
[4] A.M. EI-Nashar, I. Nusbaum, R.B. Cox, The USAID Desalination Manual United States Agency for International Development, International Desalination and Environment Association, Topsfield, 1980.
[5] K.S. Spiegler, A.D.K. Laid, Ch. 1: Thermoeconomic considerations of sea water demineralization, in: Principles of Desalination, Academic Press, New York, NY, 1980, pp. 6–36.
[6] A. Porteous, Ch. 2: Desalination Technology, Applied Science Publishers, London, 1983.
[7] B.V.D. Bruggen, Desalination by distillation and by reverse osmosis-trends towards the future, Membr. Technol. 2 (2003) 6–9.
[8] A.D. Khawaji, I.K. Kutubkhanah, J. Wie, Advances in seawater desalination technologies, Desalination 221 (2008) 47–69.
[9] P. Palenzuela, D. Alarcon, J. Blanco, E. Guillén, M. Ibarra, G. Zaragoza, Modeling of the heat transfer of a solar multi-effect distillation plant at the Plataforma Solar de Almeria, Desalin. Water Treat. 31 (2011) 257–268.
[10] H. Mahmoudi, S.A. Abdul-Wahab, M.F.A. Goosen, S.S. Sablani, J. Perret, A. Ouagued, N. Spahis, Weather data and analysis of hybrid photovoltaic-wind power generation system adapted to a seawater greenhouse desalination unit designed for arid coastal countries, Desalination 222 (2008) 119–127.
[11] H. Mahmoudi, N. Spahis, M.F. Goosen, N. Ghaffour, N. Drouiche, A. Ouagued, Application of geothermal energy for heating and fresh water production in a brackish water greenhouse desalination unit: A case study from Algeria, Renew. Sustain. Energy Rev. 14 (2010) 512–517.
[12] H. Jouhara, N. Spahis, M.F.A. Goose, Potential of heat pipe technology in nuclear seawater desalination, Desalination 249 (2009) 1055–1061.
[13] H. Tanaka, C. Park, Distillation utilizing waste heat from a portable electric generator, Desalination 258 (2010) 136–142.
[14] P. Gao, The heat transfer characteristic of evaporation/condensation in vacuum, Northwestern Polytechnical University, Xi'an, 2008.
[15] P. Gao, L. Zhang, H. Zhang, Study on heat transfer of falling film evaporation characteristics on heat pipes in negative pressure, Desalin. Water Treat. 10 (2009) 311–316.
[16] A. Leroy, Thermodynamic properties of sea slat solution to 200°C, AIChE J. 20 (1974) 326–335.
[17] S. Yang, Convection, In: Heat Transfer, High Education Publishing Company, Beijing, 1993, pp. 171–175.